Inorg. Chem. **2008**, *47*, 9010−9020

Solution Behavior and Structural Properties of Cu(I) Complexes Featuring *m*-Terphenyl Isocyanides

Brian J. Fox, Queena Y. Sun, Antonio G. DiPasquale, Alexander R. Fox, Arnold L. Rheingold, and Joshua S. Figueroa*

Department of Chemistry and Biochemistry, University of California, San Diego, 9500 Gilman Drive, Mail Code 0358, La Jolla, California 92093-0358

Received June 14, 2008

The synthesis of the *m*-terphenyl isocyanide ligand $CNAr^{Mes2}$ (Mes = 2,4,6-$Me_3C_6H_2$) is described. Isocyanide $CNAr^{Mes2}$ readily functions as a sterically encumbering supporting unit for several Cu(I) halide and pseudo halide fragments, fostering in some cases rare structural motifs. Combination of equimolar quantities of $CNAr^{Mes2}$ and CuX (X = Cl, Br and I) in tetrahydrofuran (THF) solution results in the formation of the bridging halide complexes $(\mu\text{-X})_2[Cu(THF)(CNAr^{Mes2})]_2$. Addition of $CNAr^{Mes2}$ to cuprous chloride in a 2:1 molar ratio generates the complex $ClCu(CNAr^{Mes2})_2$ in a straightforward manner. Single-crystal X-ray diffraction has revealed $ClCu(CNAr^{Mes2})_2$ to exist as a three-coordinate monomer in the solid state. As determined by solution ^1H NMR and FTIR spectroscopic studies, monomer $ClCu(CNAr^{Mes2})_2$ resists tight binding of a third $CNAr^{Mes2}$ unit, resulting in rapid isocyanide exchange. Contrastingly, addition of 3 equiv of $CNAr^{Mes2}$ to cuprous iodide readily affords the tris-isocyanide species, $ICu(CNAr^{Mes2})_3$, as determined by X-ray diffraction. Similar coordination behavior is observed in the tris-isocyanide salt $[(THF)Cu(CNAr^{Mes2})_3]OTf$ (OTf = O_3SCF_3), which is generated upon treatment of $(C_6H_6)[Cu(OTf)]_2$ with 6 equiv of $CNAr^{Mes2}$ in THF. The disparate coordination behavior of the [CuCl] fragment relative to both [CuI] and [CuOTf] is rationalized in terms of structure and Lewis acidity of the Cu-containing fragments. The putative triflate species $[Cu(CNAr^{Mes2})_3]OTf$ itself serves as a good Lewis acid and is found to weakly bind C_6H_6 in an η^1-*C* manner in the solid-state. Density Functional Theory is used to describe the bonding and energetics of the η^1-*C* Cu−C_6H_6 interaction.

Introduction

As a result of their capacity to function as good σ-donors and moderate π-acids, isocyanides (C≡N−R) have enjoyed widespread use in transition metal chemistry as both supporting ligands and reactive entities.[1−3] In coordination chemistry, isocyanides are often utilized as organic surrogates of carbon monoxide (CO) since they provide a largely similar ligand field[4] but impart differing solubility and steric attributes on the resultant complex. Accordingly, homoleptic isocyanide analogues[5] of the well-known transition metal carbonyls[6] (e.g., $Mo(CO)_6$, $Fe(CO)_5$ and $Ni(CO)_4$) and carbonyl metalates[7] (e.g., $[V(CO)_6]^-$, $[Fe(CO)_4]^{2-}$ and $[Co(CO)_4]^-$) have been prepared and studied. Although the steric properties of isocyanides can be readily tuned, it is interesting to note that the vast majority of reported homoleptic isocyanide complexes feature coordination numbers identical to, or higher than, their carbonyl analogues. This observation

* To whom correspondence should be addressed. E-mail: jsfig@ucsd.edu.

(1) Malatesta, L.; Bonati, F. *Isocyanide Complexes of Transition Metals*; Wiley: New York, 1969.
(2) Yamamoto, Y. *Coord. Chem. Rev.* **1980**, *32*, 193–233.
(3) Bonati, F.; Minghetti, G. *Inorg. Chim. Acta* **1974**, *9*, 95–112.
(4) Sarapu, A. C.; Fenske, R. F. *Inorg. Chem.* **1974**, *14*, 247–253.
(5) Weber, L. *Angew. Chem., Int. Ed.* **1998**, *37*, 1515–1517.
(6) $Mo(CNR)_6$: R = Ph; Mann, K. R.; Cimolino, M.; Geoffroy, G. L.; Hammond, G. S.; Orio, A. A.; Albertin, G.; Gray, H. B. *Inorg. Chim. Acta* **1976**, *16*, 97–101; R = *t*-Bu. (a) Chiu, K. W.; Jones, R. A.; Wilkinson, G.; Galas, A. M. R.; Hursthouse, M. B. *J. Chem. Soc., Dalton Trans.* **1981**, 2088–2097. (b) Carnahan, E. M.; Lippard, S. J. *J. Chem. Soc., Dalton Trans.* **1991**, 699–706. R = 2,6-$Me_2C_6H_3$ (Xyl); Yamamoto, Y.; Yamazaki, H. *J. Organomet. Chem.* **1985**, *282*, 191–200. $Fe(CNt\text{-}Bu)_5$: Bassett, J.-M.; Berry, D. E.; Barker, G. K.; Green, M.; Howard, J. A. K.; Stone, F. G. A. *J. Chem. Soc., Dalton Trans.* **1979**, 1003–1011. $Ni(CNt\text{-}Bu)_4$: Otsuka, S.; Nakamura, A.; Tatsuno, Y. *J. Am. Chem. Soc.* **1969**, *91*, 6994–6999.
(7) $[V(CNXyl)_6]^-$ (Xyl = 2,6-$Me_2C_6H_3$): Barybin, M. V.; Young, V. G., Jr.; Ellis, J. E. *J. Am. Chem. Soc.* **1998**, *120*, 429–430. (a) $[Fe(CNXyl)_4]^{2-}$: Brennessel, W. W.; Ellis, J. E. *Angew. Chem., Int. Ed.* **2007**, *46*, 598–600. (b) $[Co(CNXyl)_4]^-$: Warnock, G. F.; Cooper, N. J. *Organometallics* **1989**, *8*, 1826–1827.

10.1021/ic8010986 CCC: $40.75
Published on Web 08/30/2008

Chart 1. Some *m*-Terphenyl-Based Supporting Ligands

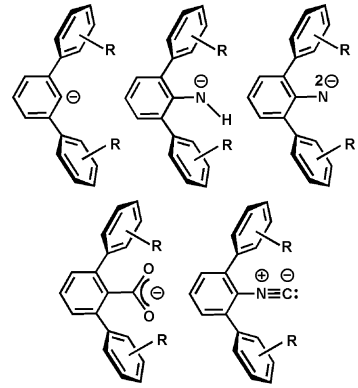

Scheme 1

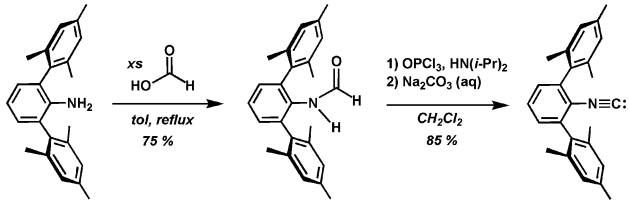

is adequately illustrated by the complexes $Mo(CN\textit{t}\text{-}Bu)_6$[6] and $K[Co(CNXyl)_4]$ (Xyl = 2,6-$Me_2C_6H_3$),[7] in which the metal coordination number is the same as that found in the carbonyl analogue despite the presence of several relatively encumbering *tert*-butyl or *m*-xylyl substituents. Correspondingly, the complexes $[Mo(CN\textit{t}\text{-}Bu)_7][PF_6]_2$[8] and $[Ta(CNXyl)_7][BF_4]$[9] represent examples in which isocyanide complexes exhibit coordination numbers greater than those found in typical metal carbonyl species.

With the aim of generating low-coordinate, coordinatively unsaturated isocyanide metal complexes, we have elected to explore the coordination chemistry of isocyanide ligands featuring the sterically encumbering *m*-terphenyl group (Chart 1).[10] This choice is inspired in part by the use of *m*-terphenyl groups by Power,[11] Robinson,[12] and others[13] for the stabilization of low-coordinate main group and transition metal species of unique bonding and composition. Whereas substituted *m*-terphenyl monoanions[11,12] and their amido,[14−17] imido,[16,18] and carboxylate[19,20] derivatives have gained prominence as sterically encumbering ancillary ligands, the neutral isocyano modification has received considerably less attention as a ligating species. Indeed, in only two reports have *m*-terphenyl isocyanides been employed as ligands for transition metals. Nagashima and coworkers[21] have reported the use of *m*-terphenyl isocyanides in conjunction with divalent nickel halides for the polymerization of ethylene, while Ito and Sawamura[22] have explored their use for the Rh-catalyzed hydrosilylation of ketones.

Notably, despite these accounts, the structural chemistry of complexes featuring such encumbering isocyanides has not been described. This information is particularly desirable given that the *m*-terphenyl framework may be reasonably expected to obviate the formation of high-coordinate complexes. Accordingly, in this paper we present the synthesis of the *m*-terphenyl isocyanide derivative $CNAr^{Mes2}$ (Mes = 2,4,6-$Me_3C_6H_2$) and detail the solution and structural behavior of several copper(I) halide complexes derived from it. The selection of Cu(I) centers as a suitable coordination platform stems from the fact that complexes of the type $XCu(CNR)_n$ (X = halide or pseudohalide) are a well-known class of ionic and molecular species,[23,24] which have found

(8) Carnahan, E. M.; Protasiewicz, J. D.; Lippard, S. J. *Acc. Chem. Res.* **1993**, *26*, 90–97; and references therein.
(9) Barybin, M. V.; Brennessel, W. W.; Kucera, B. E.; Minyaev, M. E.; Sussman, V. J.; Young, V. G., Jr.; Ellis, J. E. *J. Am. Chem. Soc.* **2007**, *129*, 1141–1150.
(10) (a) Clyburne, J. A. C.; McMullen, N. *Coord. Chem. Rev.* **2000**, *210*, 73–99. (b) Twamley, B.; Haubrich, S. T.; Power, P. P. *Adv. Organomet. Chem.* **1999**, *44*, 1–65.
(11) For example, see:(a) La Macchia, G.; Gagliardi, L.; Power, P. P.; Brynda, M. *J. Am. Chem. Soc.* **2008**, *130*, 5104–5114. (b) Rivard, E.; Power, P. P. *Inorg. Chem.* **2007**, *46*, 10047–10064. (c) Power, P. P. *Organometallics* **2007**, *26*, 4362–4372. (d) Wolf, R.; Brynda, M.; Ni, C.; Long, G. J.; Power, P. P. *J. Am. Chem. Soc.* **2007**, *129*, 6076–6077. (e) Nguyen, T.; Sutton, A. D.; Brynda, M.; Fettinger, J. C.; Long, G. J.; Power, P. P. *Science* **2005**, *310*, 844–847. (f) Power, P. P. *Chem. Commun.* **2003**, 2091–2101. (g) Phillips, A. D.; Wright, R. J.; Olmstead, M. M.; Power, P. P. *J. Am. Chem. Soc.* **2002**, *124*, 5930–5931. (h) Stender, M.; Phillips, A. D.; Wright, R. J.; Power, P. P. *Angew. Chem., Int. Ed.* **2002**, *41*, 1785–1787. (i) Eichler, B. E.; Power, P. P. *Angew. Chem., Int. Ed.* **2001**, *40*, 796–797. (j) Olmstead, M. M.; Simons, R. S.; Power, P. P. *J. Am. Chem. Soc.* **1997**, *119*, 11705–11706.
(12) For example, see:(a) Wang, Y.; Robinson, G. H. *Organometallics* **2007**, *26*, 2–11. (b) Wang, Y.; Quillian, B.; Wannere, C. S.; Wei, P.; Schleyer, P. v. R.; Robinson, G. H. *Organometallics* **2007**, *26*, 3054–3056. (c) Yang, X.-J.; Wang, Y.; Quillian, B.; Wei, P.; Chen, Z.; Schleyer, P. v. R.; Robinson, G. H. *Organometallics* **2006**, *25*, 925–929. (d) Wang, Y.; Quillian, B.; Yang, X.-J.; Wei, P.; Chen, Z.; Wannere, C. S.; Schleyer, P. v. R.; Robinson, G. H. *J. Am. Chem. Soc.* **2005**, *127*, 7672–7673. (e) Robinson, G. H. *Chem. Commun.* **2000**, 2175–2181. (f) Robinson, G. H. *Acc. Chem. Res.* **1999**, *32*, 773–782. (g) Su, J.; Li, X.-W.; Crittendon, R. C.; Campana, C. F.; Robinson, G. H. *Organometallics* **1997**, *16*, 4511–4513.
(13) For some representative recent applications, see:(a) Filippou, A. C.; Weidemann, N.; Philippopoulos, A. I.; Schnakenburg, G. *Angew. Chem., Int. Ed.* **2006**, *45*, 5987–5991. (b) Filippou, A. C.; Weidemann, N.; Schnakenburg, G.; Rohde, H.; Philippopoulos, A. I. *Angew. Chem., Int. Ed.* **2004**, *43*, 6512–6516. (c) Smith, R. C.; Gantzel, P.; Rheingold, A. L.; Protasiewicz, J. D. *Organometallics* **2004**, *23*, 5124–5126. (d) Filippou, A. C.; Philippopoulos, A. I.; Schnakenburg, G. *Organometallics* **2003**, *22*, 3339–3341. (e) Smith, R. C.; Shah, S.; Urnezius, E.; Protasiewicz, J. D. *J. Am. Chem. Soc.* **2003**, *125*, 40–41. (f) Waterman, R.; Hillhouse, G. L. *Organometallics* **2003**, *22*, 5182–5184. (g) Melenkivitz, R.;(h) Mindiola, D. J.; Hillhouse, G. L. *J. Am. Chem. Soc.* **2002**, *124*, 3846–3847. (i) Shah, S.; Simpson, M. C.; Smith, R. C.; Protasiewicz, J. D. *J. Am. Chem. Soc.* **2001**, *123*, 6925–6926. (j) Smith, R. C.; Ren, T.; Protasiewicz, J. D. *Eur. J. Inorg. Chem.* **2002**, 2779–2783.
(14) Gavenonis, J.; Tilley, T. D. *Organometallics* **2002**, *21*, 5549–5563.
(15) Wright, R. J.; Steiner, J.; Beaini, S.; Power, P. P. *Inorg. Chim. Acta* **2006**, *359*, 1939–1946.
(16) Gavenonis, J.; Tilley, T. D. *J. Am. Chem. Soc.* **2002**, *124*, 8536–8537.
(17) Li, J.; Song, H.; Cui, C.; Cheng, J.-P. *Inorg. Chem.* **2008**, *47*, 3468–3470.
(18) Gavenonis, J.; Tilley, T. D. *Organometallics* **2004**, *23*, 31–43.
(19) (a) Yoon, S.; Lippard, S. J. *J. Am. Chem. Soc.* **2005**, *127*, 8386–8397. (b) Carson, E. C.; Lippard, S. J. *J. Am. Chem. Soc.* **2004**, *126*, 3412–3413. (c) Carson, E. C.; Lippard, S. J. *Inorg. Chem.* **2006**, *45*, 828–836. (d) Carson, E. C.; Lippard, S. J. *Inorg. Chem.* **2006**, *45*, 837–848.
(20) (a) Klein, D. P.; Young, V. G., Jr.; Tolman, W. B.; Que, L., Jr. *Inorg. Chem.* **2006**, *45*, 8006–8008. (b) Hagadorn, J. R.; Que, L., Jr.; Tolman, W. B. *Inorg. Chem.* **2000**, *39*, 6086–6090. (c) Hagadorn, J. R.; Que, L., Jr.; Tolman, W. B.; Prisecaru, I.; Munck, E. *J. Am. Chem. Soc.* **1999**, *121*, 9760–9761.
(21) Tanabiki, M.; Tsuchiya, K.; Kumanomido, Y.; Matsubara, K.; Motoyama, Y.; Nagashima, H. *Organometallics* **2004**, *23*, 3976–3981.
(22) Ito, H.; Kato, T.; Sawamura, M. *Chem. Lett.* **2006**, *35*, 1038–1039.

Figure 1. Molecular structure of $CNAr^{Mes2}$. Selected bond distances (Å) and angles (deg). C1−N1 = 1.158(3); N1−C2 = 1.414(3); C1−N1−C2 = 178.1(3).

Scheme 2

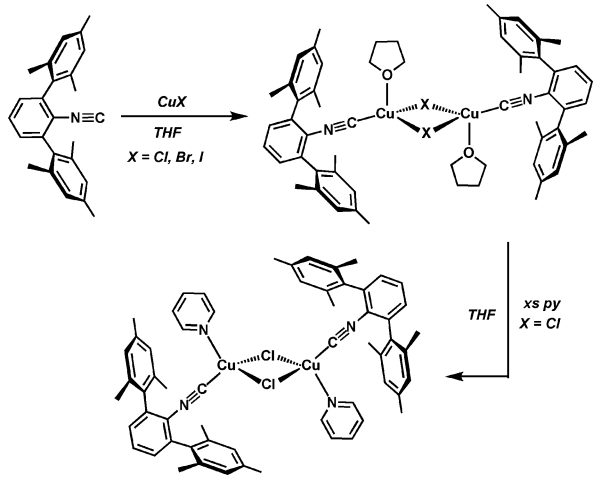

utility as reagents for organic transformations,[25] supramolecular templating agents,[26] and enzymatic probes.[27] As delineated herein, the encumbering nature of the *m*-terphenyl framework reliably controls the extent of isocyanide ligation and fosters rare structural motifs within the context of Cu(I) isocyanide chemistry.

Results and Discussion

The synthesis of *m*-terphenyl isocyanide $CNAr^{Mes2}$ is depicted in Scheme 1. Treatment of the amine H_2NAr^{Mes2} with excess formic acid readily provides the corresponding formaniline, $HC(O)N(H)Ar^{Mes2}$, in excellent yield. Dehydration of $HC(O)N(H)Ar^{Mes2}$ with $OPCl_3$ in the presence of base generates the isocyanide $CNAr^{Mes2}$ as a colorless solid after work up. Isocyanide $CNAr^{Mes2}$ has been fully characterized by ^1H and ^{13}C NMR, combustion analysis, and single crystal

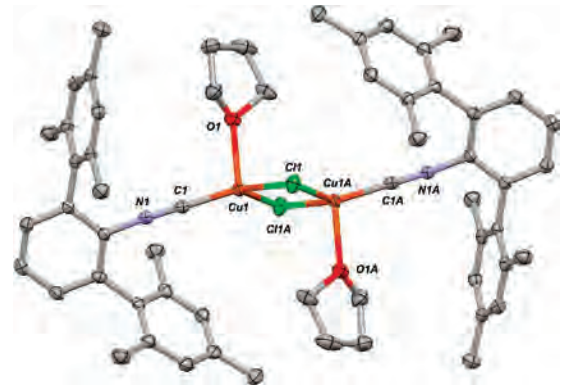

Figure 2. Molecular structure of $(\mu\text{-Cl})_2[Cu(THF)(CNAr^{Mes2})]_2$.

X-ray diffraction (Figure 1). In addition, solution (C_6D_6) and solid state (KBr) FTIR spectra of $CNAr^{Mes2}$ display intense bands at 2118 cm^{-1} and 2120 cm^{-1}, respectively, consistent with the presence of a terminal isocyano unit.

Isocyanide $CNAr^{Mes2}$ readily functions as a versatile ligand in conjunction with copper halide salts. Addition of $CNAr^{Mes2}$ to an equimolar amount of copper(I) chloride in tetrahydrofuran (THF) solution generates the bridging dichloride dimer, $(\mu\text{-Cl})_2[Cu(THF)(CNAr^{Mes2})]_2$, as determined by X-ray diffraction (Scheme 2, Figure 2, Table 1). Both the bromide and iodide congeners can be prepared in similar fashion, with crystallographic analysis of the bromide derivative (Figure 3) revealing that it is both isomorphous and isostructural to $(\mu\text{-Cl})_2[Cu(THF)(CNAr^{Mes2})]_2$. The solid-state FTIR spectra of complexes $(\mu\text{-X})_2[Cu(THF)(CNAr^{Mes2})]_2$ display isocyano stretches of 2143 cm^{-1}, 2139 cm^{-1}, and 2146 cm^{-1} for the chloride, bromide, and iodide derivatives, respectively, showing a modest shift to higher energy relative to that of free $CNAr^{Mes2}$. This later observation is consistent with the spectroscopic behavior of other organoisocyanides upon coordination to monovalent group 11 metals[28] and is interpreted to arise from stabilization of the filled isocyano σ^* orbital in the absence of significant π back-donation.[4,28−31] Accordingly, the crystallographically determined C≡N bond distances in complexes $(\mu\text{-X})_2[Cu(THF)(CNAr^{Mes2})]_2$ are not elongated relative to free $CNAr^{Mes2}$ within experimental error and the respective $C{\equiv}N{-}C_{ipso}$ angles do not significantly deviate from linearity (Table 1).

An interesting structural characteristic of complexes $(\mu\text{-X})_2[Cu(THF)(CNAr^{Mes2})]_2$, however, is the noticeably obtuse C(1)−Cu(1)−Cu(1a) angles relating the *anti*-disposed $CNAr^{Mes2}$ ligands (155.37(6)° and 153.85(10)° for the Cl and Br derivatives, respectively). This relatively large spacing between isocyanide ligands in complexes $(\mu\text{-X})_2[Cu(THF)(CNAr^{Mes2})]_2$ is proposed to manifest from the weak σ-donating capacity of THF, rather than from steric pressures associated with Ar^{Mes2} units. Lending credence to this notion is the finding that pyridine (py) readily displaces the

(23) For representative early accounts, see: (a) Irving, H.; Jonason, M. *J. Chem. Soc.* **1960**, 2095–2097. (b) Fisher, P. J.; Taylor, N. E.; Harding, M. M. *J. Chem. Soc.* **1960**, 2303–2309. (c) Otsuka, S.; Mori, K; Yamagami, K. *J. Org. Chem.* **1966**, *31*, 4170–4174. (d) Bailey, J.; Mays, M. J. *J. Organomet. Chem.* **1973**, *47*, 217–224.
(24) Bell, A.; Walton, R. A.; Edwards, D. A.; Poulter, M. A. *Inorg. Chim. Acta* **1985**, *104*, 171–178.
(25) For example:(a) Kamijo, S.; Kanazawa, C.; Yamamoto, Y. *J. Am. Chem. Soc.* **2005**, *127*, 9260–9266. (b) Fiaschi, P.; Floriani, C.; Pasquali, M.; Chiesi-Villa, A.; Guastini, C. *Inorg. Chem.* **1986**, *25*, 462–469. (c) Wakselman, C.; Tordeux, M. *J. Org. Chem.* **1979**, *44*, 4219–4220. (d) Tsuda, T.; Habu, H.; Horiguchi, S.; Saegusa, T. *J. Am. Chem. Soc.* **1974**, *96*, 5930–5931.
(26) (a) Benouazzane, M.; Coco, S.; Espinet, P.; Barbera, J. *Inorg. Chem.* **2002**, *41*, 5754–5759. (b) Benouazzane, M.; Coco, S.; Espinet, P.; Barbera, J. *J. Mater. Chem.* **2001**, *11*, 1740–1744.
(27) Reedy, B. J.; Murthy, N. N.; Karlin, K. D.; Blackburn, N. J. *J. Am. Chem. Soc.* **1995**, *117*, 9826–9831.
(28) Robertson, M. J.; Angelici, R. J. *Langmuir* **1994**, *10*, 1488–1492.
(29) Shih, K.; Angelici, R. J. *Langmuir* **1995**, *11*, 2539–2546.
(30) Henderson, J. I.; Feng, S.; Bein, T.; Kubiak, C. P. *Langmuir* **2000**, *16*, 6183–6187.
(31) Hattori, R.; Suzuki, E.; Shimizu, K. *J. Mol. Struct.* **2005**, *738*, 165–170.

Table 1. Selected Bond Distances (Å) and Angles (deg) for $(\mu\text{-Cl})_2[\text{Cu(THF)(CNAr}^{\text{Mes2}})]_2$, $(\mu\text{-Br})_2[\text{Cu(THF)(CNAr}^{\text{Mes2}})]_2$, and $(\mu\text{-Cl})_2[\text{Cu(py)(CNAr}^{\text{Mes2}})]_2$

$(\mu\text{-Cl})_2[\text{Cu(THF)(CNAr}^{\text{Mes2}})]_2$	
C1−N1	1.165(2)
C1−Cu1	1.829(2)
Cu1−Cl1	2.3525(6)
Cu1−O1	2.1912(14)
Cu1−Cl1A	2.3101(5)
C1−N1−C2	174.4(2)
N1−C1−Cu1	173.21(19)
C1−Cu1−O1	102.68(7)
C1−Cu1−Cl1	119.26(7)
O1−Cu1−Cl1	96.22(4)
C1−Cu1−Cl1A	132.46(6)
Cl1−Cu1−Cl1A	100.534(19)
O1−Cu1−Cl1A	97.32(4)
Cu1−Cl1−Cu1A	79.466(19)
C1−Cu1−Cu1A	155.37(6)
$(\mu\text{-Br})_2[\text{Cu(THF)(CNAr}^{\text{Mes2}})]_2$	
C1−N1	1.155(4)
C1−Cu1	1.849(3)
Cu1−Br1	2.4657(5)
Cu1−O1	2.183(2)
Cu1−Br1A	2.4306(5)
C1−N1−C2	175.2(3)
N1−C1−Cu1	171.9(3)
C1−Cu1−O1	101.68(11)
C1−Cu1−Br1	116.58(10)
O1−Cu1−Br1	98.33(6)
C1−Cu1−Br1A	129.91(10)
Br1−Cu1−Br1A	105.417(17)
O1−Cu1−Br1A	97.78(6)
Cu1−Br1−Cu1A	74.583(17)
C1−Cu1−Cu1A	153.85(10)
$(\mu\text{-Cl})_2[\text{Cu(py)(CNAr}^{\text{Mes2}})]_2$	
C1−N1	1.151(6)
C1−Cu1	1.854(4)
Cu1−Cl1	2.4735(15)
Cu1−N2	2.057(4)
Cu1−Cl1A	2.3183(14)
C1−N1−C2	177.3(5)
N1−C1−Cu1	170.9(5)
C1−Cu1−N2	115.13(18)
C1−Cu1−Cl1	106.46(15)
N2−Cu1−Cl	96.94(12)
C1−Cu1−Cl1A	129.76(16)
Cl1−Cu1−Cl1A	99.85(4)
N2−Cu1−Cl1A	102.90(11)
Cu1−Cl1−Cu1A	80.15(4)
C1−Cu1−Cu1A	135.01(10)

coordinated THF ligands in $(\mu\text{-Cl})_2[\text{Cu(THF)(CNAr}^{\text{Mes2}})]_2$ to provide the dimeric pyridine adduct $(\mu\text{-Cl}_2)[\text{Cu(py)(CNAr}^{\text{Mes2}})]_2$ (Scheme 2). Structural characterization of the latter (Figure 4, Table 1) reveals that pyridine induces significantly greater contraction of the corresponding C(1)−Cu(1)−Cu(1a) angle (135.01(10)°) and that this geometric distortion is readily accommodated by the $\text{CNAr}^{\text{Mes2}}$ ligands.

In contrast to the dimeric species described above, monomeric Cu(I) complexes are readily obtained when two or more $\text{CNAr}^{\text{Mes2}}$ ligands are employed. For example, combination of cuprous chloride and $\text{CNAr}^{\text{Mes2}}$ in a 1:2 molar ratio in CH_2Cl_2 solution allows for the isolation of the three-coordinate, bis-isocyanide complex $\text{ClCu(CNAr}^{\text{Mes2}})_2$ (Scheme 3). Addition of a second molar equivalent of cuprous chloride to $\text{ClCu(CNAr}^{\text{Mes2}})_2$ in THF generates $(\mu\text{-Cl})_2[\text{Cu(THF)(CNAr}^{\text{Mes2}})]_2$ as determined by ^{1}H NMR spectroscopy, thus indicating that CNAr^{Mes} participates in ligand redistribution

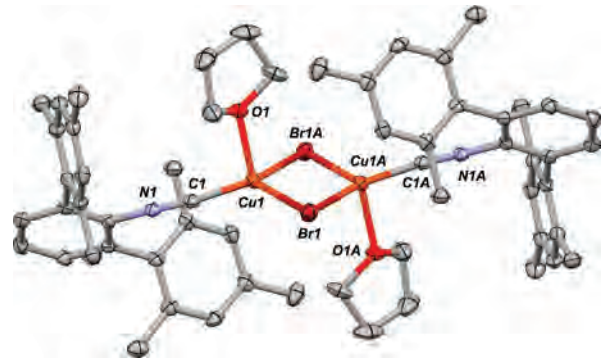

Figure 3. Molecular structure of $(\mu\text{-Br})_2[\text{Cu(THF)(CNAr}^{\text{Mes2}})]_2$.

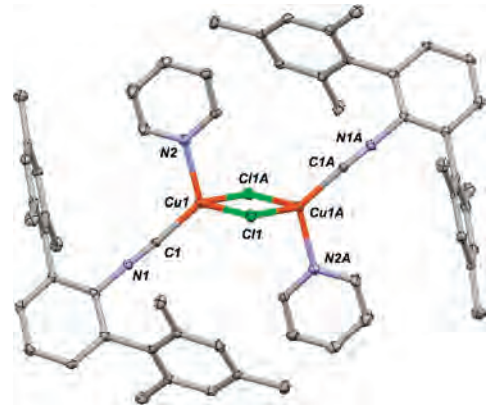

Figure 4. Molecular structure of $(\mu\text{-Cl})_2[\text{Cu(py)(CNAr}^{\text{Mes2}})]_2$.

Scheme 3

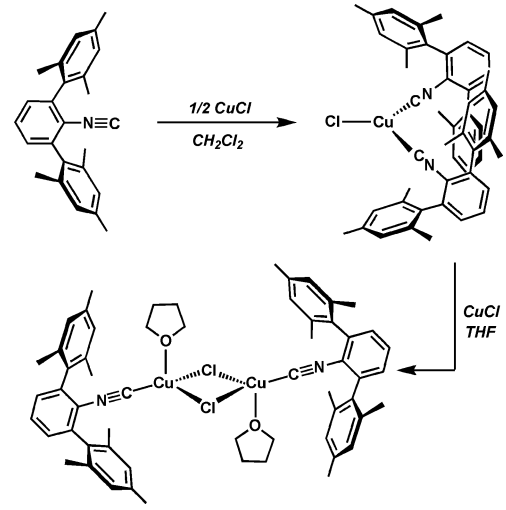

reactions under suitable conditions. Like the dinuclear Cu(I) complexes discussed above, $\text{ClCu(CNAr}^{\text{Mes2}})_2$ gives rise to an intense FTIR ν(CN) stretch centered at 2143 cm^{-1}, which is slightly higher in energy than that found for free $\text{CNAr}^{\text{Mes2}}$. The molecular structure of $\text{ClCu(CNAr}^{\text{Mes2}})_2$ has been determined by X-ray diffraction and is shown in Figure 5. The most interesting structural aspects of $\text{ClCu(CNAr}^{\text{Mes2}})_2$ are its trigonal planar coordination geometry and the perpendicular disposition of the Ar^{Mes2} central aryl rings with respect to the Cu-containing plane. As visualized from space-filling models of $\text{ClCu(CNAr}^{\text{Mes2}})_2$ (Figure 6), this latter attribute results in a substantial steric shield around roughly one-third of the Cu primary coordination sphere. However,

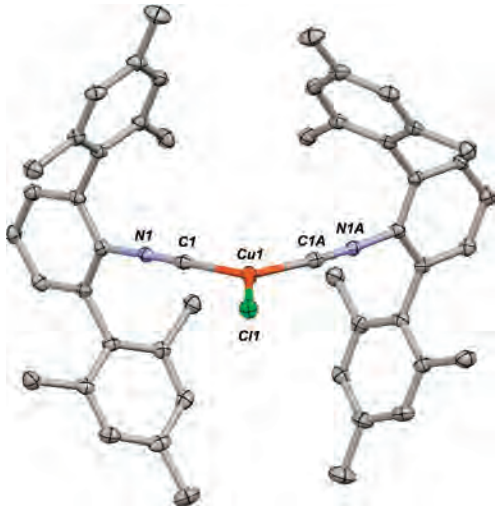

Figure 5. Molecular structure of $ClCu(CNAr^{Mes2})_2$. Selected bond distances (Å) and angles (deg): C1−N1 = 1.160(2); Cu1−C1 = 1.8993(17); Cu1−Cl1 = 2.2445(6); C1−N1−C2 = 176.60(15); C1−Cu1−C1A = 120.85(10); C1−Cu1−Cl1 = 119.58(5); C1A−Cu1−Cl1 = 119.58(5).

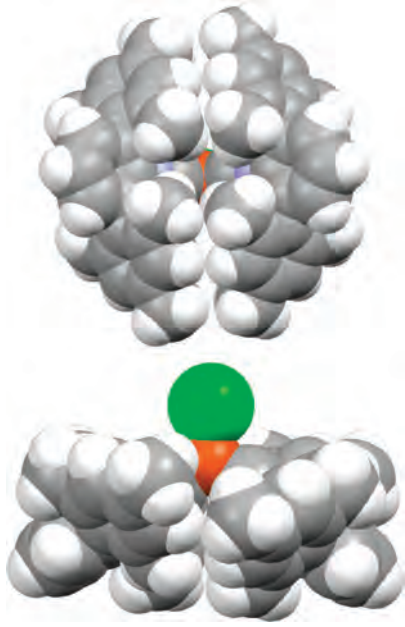

Figure 6. Space filling diagrams of $ClCu(CNAr^{Mes2})_2$. Top: View orthogonal to the trigonal plane. Bottom: View of the steric shield provided by the two Ar^{Mes2} units. Orange = Cu, Green = Cl.

despite the seemingly close-packed nature of the isocyanide ligands in $ClCu(CNAr^{Mes2})_2$, hindered rotation of the Ar^{Mes2} residues is not observed on the ^1H NMR time scale at 20 °C in C_6D_6 or at −60 °C in CD_2Cl_2 solution.

Interestingly, $ClCu(CNAr^{Mes2})_2$ represents a very rare example of a structurally authenticated monomeric bis-isocyanide Cu(I) halide complex. Indeed, most related Cu bis-isocyanide examples contain the $(\mu$-halide$)_2$ functionality in the solid state.[32,33] Only recently have Bowmaker and co-workers[34] reported the structure of $ClCu(CNt\text{-}Bu)_2$, which is the first example of a structurally characterized monomeric, $XCu(CNR)_2$ (X = halide) species. However, this complex was obtained as a byproduct in very low yield during the synthesis of the tetrakis-isocyanide salt $[Cu(CNt\text{-}Bu)_4]Cl$, and a straightforward synthesis has not been disclosed. We therefore suggest that the reliable synthesis and isolation of monomeric $ClCu(CNAr^{Mes2})_2$ in bulk can be reasonably attributed to the steric properties of the $CNAr^{Mes}$ ligand.

Scheme 4

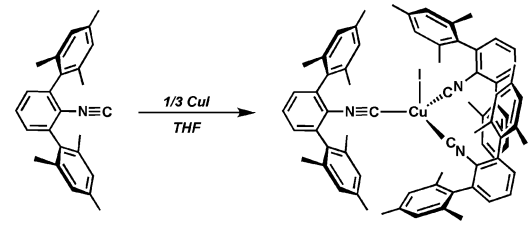

Whereas $ClCu(CNAr^{Mes2})_2$ is amenable to isolation, a third $CNAr^{Mes2}$ ligand is not readily accommodated by the [CuCl] fragment. Room temperature ^1H NMR spectra of CD_2Cl_2 solutions containing equimolar quantities of $ClCu(CNAr^{Mes2})_2$ and $CNAr^{Mes2}$ exhibit sharp resonances at chemical shifts corresponding to the weighted average of the two species. Analogous spectroscopic behavior is observed for 1:2 $ClCu(CNAr^{Mes2})_2/CNAr^{Mes2}$ mixtures in the same solvent, strongly indicating rapid exchange of free and coordinated $CNAr^{Mes2}$ on the ^1H NMR time scale. In accord with the kinetic lability of the d^{10} Cu(I) ion,[35] ligand exchange in this system is facile as demonstrated by the finding that the composite Ar^{Mes2} resonances in 1:1 $ClCu(CNAr^{Mes2})_2/CNAr^{Mes2}$ mixtures first begin to broaden at −40 °C when assayed by ^1H NMR spectroscopy (CD_2Cl_2). Isocyanide exchange is further corroborated by FTIR spectroscopy. Room temperature C_6D_6 solutions containing equal quantities of $ClCu(CNAr^{Mes2})_2$ and $CNAr^{Mes2}$ exclusively exhibit distinct ν_{CN} stretches attributable to both species, with no spectroscopic evidence for the formation of a new complex. However, it is important to note that free $CNAr^{Mes2}$ is not observed in the FTIR spectrum of pure $ClCu(CNAr^{Mes2})_2$ in C_6D_6 solution. This latter detail suggests that $ClCu(CNAr^{Mes2})_2$ retains its integrity in solution and does not readily undergo ligand redistribution or exchange reactions in the absence of an additional cuprous chloride or $CNAr^{Mes2}$. As pointed out by Floriani, [32] the inherent lability of the Cu(I)-isocyanide linkage leads to complex $[Cu(CNR)_n]_x$ speciation patterns in solution. For this $Cu(I)/CNAr^{Mes2}$ system, however, well-defined complexes are available in solution when agents which may induce ligand redistribution or exchange are not present.

Unlike cuprous chloride, addition of 3 equiv of $CNAr^{Mes2}$ to cuprous iodide affords the isolable tris-isocyanide complex $ICu(CNAr^{Mes2})_3$ under straightforward synthetic conditions (Scheme 4). In solution at 20 °C, $ICu(CNAr^{Mes2})_3$ gives rise

(32) Toth, A.; Floriani, C.; Chiesi-Villa, A.; Gaustini, C. *J. Chem. Soc., Dalton Trans.* **1988**, 1599–1605.
(33) Reference 25a reports several examples of $(\mu$-X$)_2[Cu(CNR)_2]_2$ complexes (X = Cl, Br, I) proposed on the basis of powder X-ray diffraction experiments.
(34) Bowmaker, G. A.; Hanna, J. V.; Hahn, F. E.; Lipton, A. S.; Oldham, C. E.; Skelton, B. W.; Smith, M. E.; White, A. H. *Dalton Trans.* **2008**, 1710–1720.
(35) (a) Frei, U. M.; Geier, G. *Inorg. Chem.* **1992**, *31*, 187–190. (b) Frei, U. M.; Geier, G. *Inorg. Chem.* **1992**, *31*, 3132–3137.

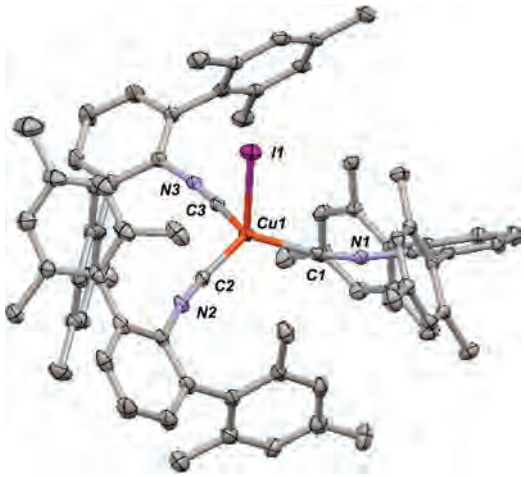

Figure 7. Molecular structure of $ICu(CNAr^{Mes2})_3$. Selected bond distances (Å) and angles (deg) for $ICu(CNAr^{Mes2})_3$. Cu1−C1 = 1.941(3); Cu1−C2 = 1.933(3); Cu1−C3 = 1.942(3); C1−N1 = 1.164(3); C2−N2 = 1.154(3); C3−N3 = 1.160(3); C1−Cu1−C2 = 115.51(11); C1−Cu1−C3 = 117.18(10); C2−Cu1−C3 = 115.93(10); C1−Cu1−I1 = 101.73(7); C2−Cu1−I1 = 102.40(8); C3−Cu1−I1 = 100.02(8).

Scheme 5

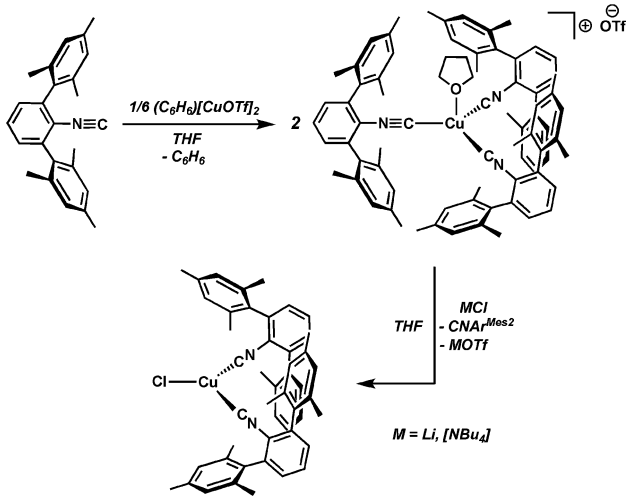

to a single set of Ar^{Mes2} resonances in its ^1H NMR spectrum which remains sharp down to −60 °C (CD_2Cl_2). Thus, $CNAr^{Mes2}$ dissociation does not appear to be taking place at ambient or cooler temperatures. As depicted in Figure 7, $ICu(CNAr^{Mes2})_3$ exists as a pseudo C_3-symmetric monomer in the solid state by virtue of the propeller-like arrangement of its three Ar^{Mes2} residues. The important Cu-based metric parameters for $ICu(CNAr^{Mes2})_3$ match well with the iodo tris-isocyanide complex, $ICu(CN(p\text{-Tol}))_3$,[32] signifying that the encumbering Ar^{Mes2} groups do not impart a ligand-enforced geometry on the Cu center. Accordingly, the Cu coordination geometry in $ICu(CNAr^{Mes2})_3$ is best described as intermediate between tetrahedral and trigonal pyramidal extremes. Calculation of Houser's τ_4 four-coordinate geometry index[36] supports this claim and results in a value of 0.90 for $ICu(CNAr^{Mes2})_3$, which is conservatively midrange between idealized tetrahedral (τ_4 = 1.0) and trigonal pyramidal (τ_4 = 0.85). While subtle, we speculate that this distortion

(36) Yang, L.; Powell, D. R.; Houser, R. P. *Dalton Trans.* **2007**, 955–964.

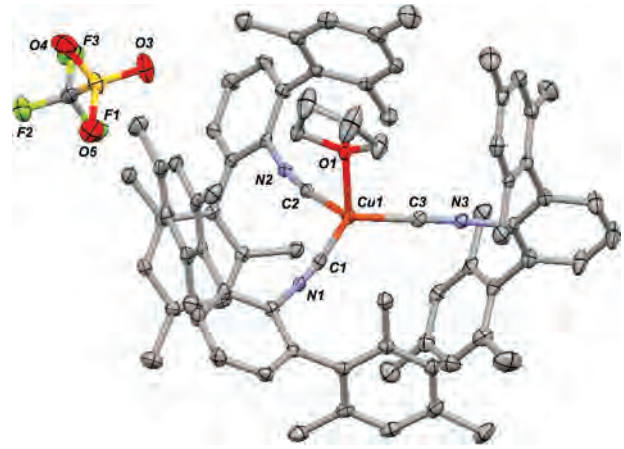

Figure 8. Molecular structure of $[(THF)Cu(CNAr^{Mes2})_3]OTf$. Selected bond distances (Å) and angles (deg): Cu1−C1 = 1.931(3); Cu1−C2 = 1.921(3); Cu1−C3 = 1.916(3); Cu1−O1 = 2.182(2); C1−N1 = 1.148(4); C2−N2 = 1.159(4); C3−N3 = 1.154(4); C1−Cu1−C2 = 117.50(13); C1−Cu1−C3 = 119.04(13); C2−Cu1−C3 = 119.14(13); O1−Cu1−C1 = 96.06(11); O1−Cu1−C2 = 95.54(11); O1−Cu1−C3 = 99.21(11).

reflects a snapshot along the continuum of dissociation of the I−Cu(I) unit consistent with the ability of iodide to serve as a good leaving group.

To this end, utilization of triflate ($[F_3CSO_3]^-$, OTf) in place of iodide leads to a tris-isocyanide complex in which the anion is fully dissociated. Thus, treatment of $(C_6H_6)[Cu(OTf)]_2$ with 6.0 equiv of $CNAr^{Mes2}$ in THF (Scheme 5) readily provides the tris-isocyanide THF adduct, $[(THF)Cu(CNAr^{Mes2})_3]OTf$, as a well-separated cation/anion pair (Figure 8). Calculation of the τ_4 parameter for $[(THF)Cu(CNAr^{Mes2})_3]OTf$ results in a value of 0.86, which is clearly indicative of a trigonal pyramidal four-coordinate geometry and reflects the inability of THF to significantly pyramidalize the $[Cu(CNR)_3]^+$ core. Furthermore, simple addition of $CNAr^{Mes2}$ to $(C_6H_6)[CuOTf]_2$ does not generate a tetrakis-isocyanide Cu(I) derivative despite the weakly coordinating nature of the triflate anion. This observation signifies that the $CNAr^{Mes2}$ ligand can foster low-coordinate species under suitable conditions since complexes of the type $[Cu(CNR)_4]X$ are commonly encountered with less encumbering isocyanides.[32,34,37,38]

The fact that both cuprous iodide and cuprous triflate afford tris-$CNAr^{Mes2}$ complexes, while cuprous chloride does not, is particularly curious. To ascertain whether a tris-isocyanide chloride complex is inherently destabilized in conjunction with $CNAr^{Mes2}$, the triflate species $[(THF)Cu(CNAr^{Mes2})_3]OTf$ was treated with external chloride sources. As depicted in Scheme 5, treatment of $[(THF)Cu(CNAr^{Mes2})_3]OTf$ with either LiCl or $[NBu_4]Cl$ in THF solution generates $ClCu(CNAr^{Mes2})_2$ concomitant with the release of a $CNAr^{Mes2}$ ligand.[39] Therefore, we propose that

(37) Knol, D.; Koole, N. J.; de Bie, M. J. A. *Org. Magn. Reson.* **1976**, *8*, 213–218.
(38) Kitagawa, S.; Munakata, M. *Inorg. Chem.* **1984**, *23*, 4388–4390.
(39) Data in support of $CNAr^{Mes2}$ ejection from copper upon chloride ligation include ^1H NMR and FTIR spectra (solution and solid-state) that are identical to those produced in the isocyanide exchange studies outlined above. In addition, an $^{19}F\{^1H\}$ NMR signal is not observed from the C_6D_6 soluble fraction after $[(THF)Cu(CNAr^{Mes2})_3]OTf$ is treated with LiCl.

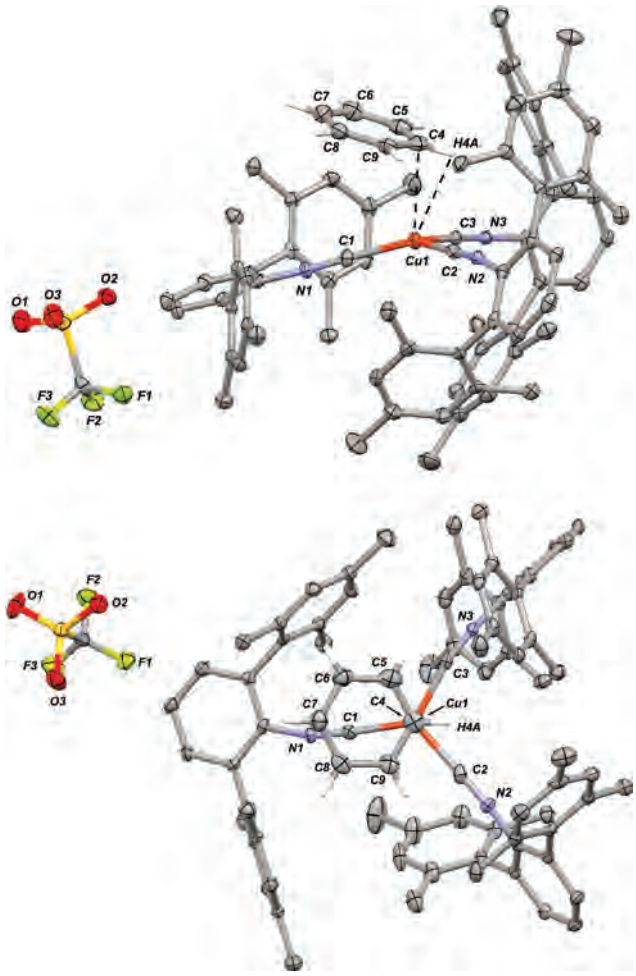

Figure 9. Molecular structure of $[(\eta^1\text{-}C\text{-}C_6H_6)Cu(CNAr^{Mes2})_3]OTf$. Top: perspective view. Bottom: View down the pseudo 3-fold axis of the $[Cu(CNAr^{Mes2})_3]$ fragment. Hydrogen atoms of the $[Cu(CNAr^{Mes2})_3]$ fragment have been omitted for clarity. Selected bond distances (Å) and angles (deg). Cu1−C4 = 2.715(5); Cu1−H4A = 2.659(5); Cu1−C5 = 3.194(5); Cu1−C9 = 3.165(5); Cu1−C1 = 1.921(5); Cu1−C2 = 1.923(5); Cu1−C3 = 1.939(4); $d(C{\equiv}N)_{av}$ = 1.159 ± 0.009; C4−C5 = 1.378(7); C4−C9 = 1.369(7); $d(C{-}C, C_6H_6)_{av}$ = 1.373 ± 0.009; C1−Cu1−C2 = 122.00(19); C1−Cu1−C3 = 121.69(18); C2−Cu1−C3 = 111.44(18).

tight binding of a third $CNAr^{Mes2}$ ligand to $ClCu(CNAr^{Mes2})_2$ is disfavored as a result of the attenuated Lewis acidity of the [CuCl] fragment relative to either [CuI][40] or [CuOTf],[41] rather than steric inaccessibility posed by the Ar^{Mes2} residues. Accordingly, it has been noted that [CuI] and [CuOTf] salts can function as more efficient Lewis acid catalysts for organic transformations than their [CuCl] analogues.[41,42]

With respect to the Lewis acidity of the $[Cu(CNAr^{Mes2})_3]^+$ fragment, it is notable that crystallization of putative $[[Cu(CNAr^{Mes2})_3]OTf]$ from dilute C_6H_6 solution afforded a species which, in the solid state, may reasonably be described as possessing a weak η^1-*C* Cu-benzene interaction.[43] As shown in Figure 9 (top), the C_6H_6 molecule in $[(\eta^1\text{-}C\text{-}C_6H_6)Cu(CNAr^{Mes2})_3]OTf$ docks at an angle within the protective framework of the three $CNAr^{Mes2}$ ligands. A view down the pseudo 3-fold axis reveals that only one carbon atom is situated directly over the Cu center (Figure 9, bottom). Whereas several η^2-arene complexes of Cu(I) are known,[44−50] η^1-*C* coordination has not previously been established for a Cu center and is rare in general.[51−58] Furthermore, of the η^1-*C* arene-metal interactions structurally verified, only two examples[51,53] exist in which the arene unit is unsupported by a larger ligand framework. Although the Cu−C4 bond length of 2.715 Å in $[(\eta^1\text{-}C\text{-}C_6H_6)\text{-}Cu(CNAr^{Mes2})_3]OTf$ is long when compared to other structurally characterized η^1-*C* arene complexes, aspects of its structure point to the existence of a weak interaction between C_6H_6 and the central Cu atom. These include (i) the angular canting of C4 and H4A in the direction of the Cu center and (ii) the concomitant slight pyramidalization of the Cu center in the direction opposite of the C_6H_6 molecule ($\Sigma(\angle C_{iso}{-}Cu{-}C_{iso})$ = 355.14°). In addition, one Ar^{Mes2} residue is observed to rotate orthogonally to the other two, seemingly adjusting to accommodate the presence of the C_6H_6 molecule. Taken together, these structural attributes reflect an electronic and steric perturbation of the $[Cu(C\text{-}NAr^{Mes2})_3]^+$ core which would not be expected simply from a C_6H_6 molecule of co-crystallization.

To further probe the close Cu−C_6H_6 contact in $[(\eta^1\text{-}C\text{-}C_6H_6)Cu(CNAr^{Mes2})_3]OTf$, the computational model $[(\eta^1\text{-}C\text{-}C_6H_6)Cu(CNAr^{Ph2})_3]^+$ was studied using density functional theory (DFT). As shown in Figure 10, the optimized structure of $[(\eta^1\text{-}C\text{-}C_6H_6)Cu(CNAr^{Ph2})_3]^+$ matches well with its experimental counterpart and does not converge to an η^2-C_6H_6 minimum. Furthermore, the C_6H_6 unit remains angled and within close proximity to the Cu center. Analysis of the electronic structure of $[(\eta^1\text{-}C\text{-}C_6H_6)Cu(CNAr^{Ph2})_3]^+$ does reveal a low-lying filled molecular orbital (HOMO-22) indicative of bonding between Cu and the proximal carbon atom of the C_6H_6 molecule (Figure 11). Also apparent is that a binodal, e_{1g}-type orbital is used by C_6H_6 to bind to the Cu center. Most interestingly, the p-orbital coefficients

(40) Singh, P. P.; Srivatava, S. K.; Srivatava, A. K. *J. Inorg. Nucl. Chem.* **1980**, *42*, 521–532.
(41) Yamamoto, Y. *J. Org. Chem.* **2007**, *72*, 7817–7831.
(42) Ma, B.; Snyder, J. K. *Organometallics* **2002**, *21*, 4688–4695.
(43) Hubig, S. M.; Lindeman, S. V.; Kochi, J. K. *Coord. Chem. Rev.* **2000**, *200*, 831–873.
(44) Turner, R. W.; Amma, E. L. *J. Am. Chem. Soc.* **1963**, *85*, 4046–4047.
(45) Dines, M. B.; Bird, P. H. *J. Chem. Soc., Chem. Commun.* **1973**, *1*, 12–12.
(46) Rodesiler, P. F.; Amma, E. L. *J. Chem. Soc. Chem. Commun.* **1974**, 599–600.
(47) Dattelbaum, A. M.; Martin, J. D. *Inorg. Chem.* **1999**, *38*, 6200–6205.
(48) Laitar, D. S.; Mathison, C. J. N.; Davis, W. M.; Sadighi, J. P. *Inorg. Chem.* **2003**, *42*, 7354–7356.
(49) Hamilton, C. W.; Laitar, D. S.; Sadighi, J. P. *Chem. Commun.* **2004**, 1628–1629.
(50) Amisial, L. D.; Dai, X.; Kinney, R. A.; Krishnaswamy, A.; Warren, T. H. *Inorg. Chem.* **2004**, *43*, 6537–6539.
(51) Lau, W.; Huffman, J. C.; Kochi, J. K. *J. Am. Chem. Soc.* **1982**, *104*, 5515–5517.
(52) Chen, H.; Bartlett, R. A.; Olmstead, M. M.; Power, P. P.; Shoner, S. C. *J. Am. Chem. Soc.* **1990**, *112*, 1048–1055.
(53) Batsanov, A. S.; Crabtree, S. P.; Howard, J. A. K.; Lehmann, C. W.; Kilner, M. *J. Organomet. Chem.* **1998**, *550*, 59–61.
(54) Albrecht, M.; Spek, A. L.; van Koten, G. *J. Am. Chem. Soc.* **2001**, *123*, 7233–7246.
(55) Geldbach, T. J.; Drago, D.; Pregosin, P. S. *J. Organomet. Chem.* **2002**, *643*, 214–222.
(56) Reid, S. M.; Boyle, R. C.; Mague, J. T.; Fink, M. J. *J. Am. Chem. Soc.* **2003**, *125*, 7816–7817.
(57) Krumper, J. R.; Gerisch, M.; Magistrato, A.; Rothlisberger, U.; Bergman, R. G.; Tilley, T. D. *J. Am. Chem. Soc.* **2004**, *126*, 12492–12502.
(58) Barder, T. E. *J. Am. Chem. Soc.* **2006**, *128*, 898–904.

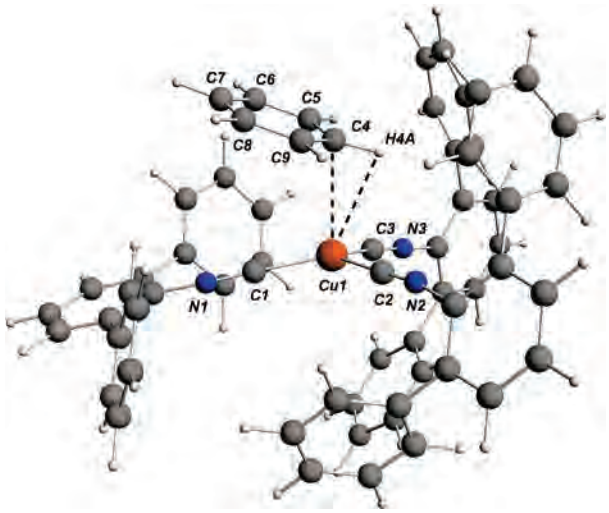

Figure 10. DFT minimized molecular structure of model $[(\eta^1\text{-}C\text{-}C_6H_6)Cu(CNAr^{Ph2})_3]^+$. Selected bond distances (Å) and angles (deg). Cu1−C4 = 2.769; Cu1−H4A = 2.713; Cu1−C5 = 3.317; Cu1−C9 = 3.276; Cu1−C1 = 1.881; Cu1−C2 = 1.886; Cu1−C3 = 1.902; $d(C{\equiv}N)_{av}$ = 1.173 ± 0.005; $d(C-C, C_6H_6)_{av}$ = 1.399 ± 0.004; C1−Cu1−C2 = 122.3; C1−Cu1−C3 = 122.3; C2−Cu1−C3 = 110.4. Numbering scheme follows that of the X-ray structure for $[(\eta^1\text{-}C\text{-}C_6H_6)Cu(CNAr^{Mes2})_3]OTf$.

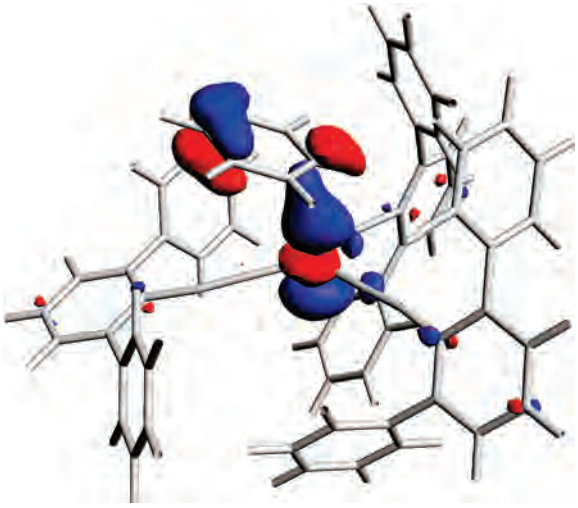

Figure 11. Molecular orbital 214 (HOMO-22) in $[(\eta^1\text{-}C\text{-}C_6H_6)Cu(CNAr^{Ph2})_3]^+$ describing the primary η^1-*C* C_6H_6−Cu bonding interaction. Isosurface value = 0.03 au.

of both "*ortho*" carbon atoms of this orbital vanish, reflecting the symmetry lowering of the C_6H_6 unit brought about by the η^1 C−Cu interaction. However, calculation of ΔH^{SCF} for the hypothetical reaction C_6H_6 + $[Cu(CNAr^{Ph2})_3]^+ \rightarrow [(\eta^1\text{-}C\text{-}C_6H_6)Cu(CNAr^{Ph2})_3]^+$ results in an enthalpic driving force of only 3.0 kcal/mol for η^1-C_6H_6 binding.[59] Thus, while manifest in the solid state, it is doubtful that such an interaction is strongly preserved in solution by the cationic $[Cu(CNAr^{Mes2})_3]^+$ fragment. Accordingly, as Tilley and co-workers[57] have shown, η^1-*C* M-arene interactions can be persistent and spectroscopically observable in solution when buttressed by the framework of a multidentate ligand.

(59) It is pertinent to note that model $[Cu(CNAr^{Ph2})_3]^+$ optimized to a structure containing a planar Cu atom ($\Sigma(\angle C_{iso}-Cu-C_{iso})$ = 359.4°, Supporting Information, Figure S2-1). This observation lends credence to the notion that the presence of a C_6H_6 molecule perturbs the Cu coordination geometry in $[(\eta^1\text{-}C\text{-}C_6H_6)Cu(CNAr^{Mes2})_3]OTf$.

In conclusion, the *m*-terphenyl isocyanide framework functions as a versatile supporting group for monovalent Cu centers. As revealed from crystallographic studies, the compliment of either two or three ligated $CNAr^{Mes2}$ units provides an effective steric shield around a central metal center. Given the portability of the isocyano moiety to large number of transition metal fragments, it is anticipated that derivatized *m*-terphenyl isocyanide ligands will engender the formation of reactive, low coordinate species capable of productive transformations of exogenous substrates.

Experimental Section

General Considerations. All manipulations were carried out under an atmosphere of dinitrogen using standard Schlenk and glovebox techniques. Solvents were dried and deoxygenated according to standard procedures. Unless otherwise stated, reagent grade starting materials were purchased from commercial sources and used as received. Benzene-d_6, methylene chloride-d_2, and chloroform-*d* (Cambridge Isotope Laboratories) were degassed and stored over 4 Å molecular sieves for 2 d prior to use. The aniline[14,15] H_2NAr^{Mes2} and $(C_6H_6)[Cu(OTf)]_2$[60] were prepared as described previously. LiCl and KBr were stirred overnight in anhydrous THF, filtered, and dried under vacuum (24 h) at a temperature above 250 °C prior to use. $[NBu_4]Cl$ was subjected to three cycles of stirring in anhydrous THF and drying in vacuo prior to use. Solution ^1H, $^{13}C\{^1H\}$ and ^{19}F NMR spectra were recorded on Varian Mercury 300 and 400 spectrometers. ^1H and ^{13}C chemical shifts are reported in ppm relative to $SiMe_4$ (^1H and ^{13}C δ = 0.0 ppm) with reference to residual solvent resonances of 7.16 ppm (^1H) and 128.06 ppm (^{13}C) for benzene-d_6, 5.32 ppm (^1H) for methylene chloride-d_2, and 7.26 ppm (^1H) and 77.1 ppm (^{13}C) for chloroform-*d*. ^{19}F NMR spectra were referenced externally to neat trifluoroacetic acid, $F_3CC(O)OH$ (δ = −78.5 ppm vs $CFCl_3$ = 0.0 ppm). FTIR spectra were recorded on a Thermo-Nicolet Avatar 380 FT-IR spectrometer as either KBr pellets or as C_6D_6 solutions in a ThermoFisher solution cell equipped with KBr windows. For solution FTIR spectra, solvent peaks were digitally subtracted from all spectra by comparison with an authentic spectrum obtained immediately prior to that of the sample. Combustion analyses were performed by Robertson Microlit Laboratories, Madison, NJ.

Synthesis of $HC(O)NHAr^{Mes2}$. To a toluene solution of H_2NAr^{Mes2} (13.45 g, 40.8 mmol, 200 mL) was added formic acid (HCOOH, 28.18 g, 612.3 mmol, 15 equiv). The resulting yellow mixture was refluxed in a Dean−Stark apparatus with periodic readdition of condensed HCOOH. After 12 h, all volatile materials were removed under reduced pressure affording $HC(O)NHAr^{Mes2}$ colorless solid, which was washed with Et_2O (3 × 20 mL) and hexanes (2 × 30 mL) before being dried in vacuo. Yield: 10.99 g, 30.7 mmol, 75.3%. ^1H NMR (300.1 MHz, $CDCl_3$, 20 °C): δ = 7.63 (d, 1H, *J* = 6 Hz, *H*C(O)NH), 7.32 (t, 1H, *J* = 7 Hz, *p*-Ph), 7.14 (d, 2H, *J* = 7 Hz, *m*-Ph), 6.96 (s, 4H, *m*-Mes), 6.60 (br d, 1H, *J* = 6 Hz, HC(O)N*H*), 2.32 (s, 6H, *p*-CH_3), 2.01 (s, 12H, *o*-CH_3) ppm. $^{13}C\{^1H\}$ NMR (100.6 MHz, $CDCl_3$, 20 °C): δ = 162.7 (*C*═O), 138.0, 135.9, 134.5, 133.4, 132.3, 130.3, 129.0, 126.0, 21.2 (*p*-CH_3), 20.4 (*o*-CH_3) ppm. FTIR (KBr pellet) (ν_{CO}) 1682 cm^{-1} also 3358 (ν_{NH}), 2972, 2912, 2854, 1612, 1492, 1456, 1410, 1377, 1276, 1207, 1178, 860, 813, 764 cm^{-1}. Anal. Calcd for $C_{25}H_{27}NO$: C, 83.99; H, 7.61; N, 3.92. Found: C, 83.74; H, 7.71; N, 3.77.

Synthesis of $CNAr^{Mes2}$. To a CH_2Cl_2 solution of $HC(O)NHAr^{Mes2}$ (9.29 g, 25.99 mmol, 150 mL) was added diisopropylamine

(60) Salomon, R. G.; Kochi, J. K. *J. Am. Chem. Soc.* **1973**, *95*, 3300–3310.

Table 2. Crystallographic Data and Refinement Information

	$CNAr^{Mes}$	$(\mu\text{-Cl})_2[Cu(THF)(CNAr^{Mes2})]_2\cdot THF$	$(\mu\text{-Br})_2[Cu(THF)(CNAr^{Mes2})]_2\cdot THF$
formula	$C_{25}H_{25}N$	$C_{62}H_{74}Cl_2Cu_2N_2O_3$	$C_{62}H_{74}Br_2Cu_2N_2O_3$
crystal system	orthorhombic	monoclinic	monoclinic
space group	*Pbca*	$P2_1/n$	$P2_1/n$
a, Å	17.304(2)	8.2737(4)	8.2999(6)
b, Å	7.9368(10)	11.4673(6)	11.6485(9)
c, Å	28.327(4)	29.3505(14)	29.157(2)
α, deg	90	90	90
β, deg	90	95.7120(10)	95.2910(10)
γ, deg	90	90	90
V, Å^3	3890.5(9)	2770.9(2)	2807.0(4)
Z	8	2	2
ρ (calcd), g/cm^3	1.159	1.310	1.399
μ (Mo Kα), mm^{-1}	0.066	0.910	2.227
θ max, deg	25.35	28.27	26.37
data/parameters	3556/242	6394/304	5748/298
R_1	0.0535	0.0398	0.0420
wR_2	0.1258	0.0922	0.1025
GOF	1.006	1.052	1.018

	$(\mu\text{-Cl})_2[Cu(py)(CNAr^{Mes2})]_2\cdot C_6H_{12}$	$ClCu(CNAr^{Mes2})_2\cdot 4CH_2Cl_2$	$ICu(CNAr^{Mes2})_3\cdot 8THF$
formula	$C_{66}H_{72}Cl_2Cu_2N_4$	$C_{54}H_{58}Cl_9CuN_2$	$C_{107}H_{139}CuIN_3O_8$
crystal system	monoclinic	monoclinic	triclinic
space group	$P2_1/n$	*C*2/*c*	$P\bar{1}$
a, Å	8.386(3)	26.8408(15)	14.5797(14)
b, Å	11.429(4)	9.1119(5)	14.8369(14)
c, Å	29.257(10)	24.5812(14)	24.492(2)
α, deg	90	90	83.6590(10)
β, deg	94.965(6)	115.0380(10)	72.7190(10)
γ, deg	90	90	85.1320(10)
V, Å^3	2793.7(17)	5446.9(5)	5020.4(8)
Z	2	4	2
ρ (calcd), g/cm^3	1.331	1.363	1.157
μ (Mo Kα), mm^{-1}	0.902	0.880	0.578
θ max, deg	25.03	28.13	26.37
data/parameters	4718/340	6170/305	20297/739
R_1	0.0775	0.0322	0.0434
wR_2	0.2004	0.0764	0.1004
GOF	1.027	1.048	0.846

	$(THF)Cu(CNAr^{Mes2})_3]OTf\cdot THF$	$[(\eta^1\text{-}C\text{-}C_6H_6)Cu(CNAr^{Mes2})_3]OTf$
formula	$C_{84}H_{91}CuF_3N_3O_5S$	$C_{82}H_{81}CuF_3N_3O_3S$
crystal system	monoclinic	orthorhombic
space group	$P2_1/n$	$P2_12_12_1$
a, Å	12.0551(9)	13.649(3)
b, Å	34.396(3)	20.164(4)
c, Å	18.6865(14)	25.500(5)
α, deg	90	90
β, deg	94.7720(10)	90
γ, deg	90	90
V, Å^3	7721.4(10)	7018(2)
Z	4	4
ρ (calcd), g/cm^3	1.183	1.239
μ (Mo Kα), mm^{-1}	0.368	0.400
θ max, deg	25.03	25.56
data/parameters	13644/892	13008/838
R_1	0.0569	0.0576
wR_2	0.1056	0.1322
GOF	1.022	1.008

(9.21 g, 91.0 mmol, 3.5 equiv). The solution was cooled to 0 °C under an N_2 atmosphere and $POCl_3$ (4.38 g, 28.6 mmol, 1.1 equiv) was added dropwise via syringe. The resulting mixture was allowed to stir for 3 h, after which 80 mL of an aqueous 1.5 M Na_2CO_3 was transferred via cannula. After an additional 12 h of stirring, the organic and aqueous layers were separated, and the latter was washed with CH_2Cl_2 (3 × 50 mL). The combined CH_2Cl_2 extracts were dried with $MgSO_4$, filtered and dried in vacuo, affording isocyanide $CNAr^{Mes2}$ as a colorless solid. Yield: 7.50 g, 22.1 mmol, 85.0%. ^{1}H NMR (500.3 MHz, C_6D_6, 20 °C): δ = 6.97 (t, 1H, J = 8 Hz, *p*-Ph), 6.85 (s, 4H, *m*-Mes), 6.84 (d, 2H, J = 8 Hz, *m*-Ph), 2.16 (s, 6H, *p*-CH_3), 2.05 (s, 12H, *o*-CH_3) ppm. $^{13}C\{^1H\}$ NMR (100.6 MHz, C_6D_6, 20 °C): δ = 170.7 (*C*≡N), 139.9, 137.8, 135.7, 134.8, 129.4, 129.3, 128.9, 95.7, 21.2 (*p*-CH_3), 20.3 (*o*-CH_3) ppm. FTIR (KBr pellet): (ν_{CN}) 2120 cm^{-1} also 2999, 2970, 2944, 2916, 2854, 1613, 1457, 1416, 1378, 862, 853, 807, 787, 760 cm^{-1}. FTIR (KBr windows, C_6D_6 solution): 2118 cm^{-1}. Anal. Calcd for $C_{25}H_{25}N$: C, 88.45; H, 7.42; N, 4.13. Found: C, 88.43; H, 7.54; N, 4.17.

Synthesis of $(\mu\text{-Cl})_2[Cu(THF)(CNAr^{Mes2})]_2$. To a THF slurry of cuprous chloride (0.036 g, 0.37 mmol, 2 mL) was added a THF solution of $CNAr^{Mes2}$ (0.125 g, 0.37 mmol, 3 mL). The mixture was stirred for 2 h before all volatile materials were removed under reduced pressure. Dissolution of the resulting colorless residue in

THF (2−3 mL) followed by filtration and storage at −35 °C for 12 h resulted in colorless crystals, which were collected and dried in vacuo. Yield: 0.210 g, 0.48 mmol, 81.3%. The coordinated THF ligands are observed to dissociate in C_6D_6 solution. ^{1}H NMR (500.3 MHz, C_6D_6, 20 °C): δ = 6.90 (t, 1H, J = 8 Hz, *p*-Ph), 6.84 (s, 4H, *m*-Mes), 6.75 (d, 2H, J = 8 Hz, *m*-Ph), 2.18 (s, 6H, *p*-CH_3), 1.94 (s, 12H, *o*-CH_3) ppm. ^{13}C{^{1}H} NMR (100.6 MHz, C_6D_6, 20 °C): δ = 148.9 (*C*≡N), 140.3, 138.4, 135.3, 133.7, 129.7, 129.4, 129.2, 126.6, 21.4 (*p*-*C*H_3), 20.2 (*o*-*C*H_3) ppm. FTIR (KBr pellets) (ν_{CN}) 2143 cm^{-1} also 2947, 2917, 2856, 1613, 1456, 1376, 851, 805, 756 cm^{-1}. Prolonged drying in vacuo resulted in an analytically pure sample lacking coordinated THF. Anal. Calcd for $C_{25}H_{25}NCuCl$: C, 68.48; H, 5.75; N, 3.19. Found: C, 68.48; H, 5.83; N, 3.11. Addition of several drops of pyridine (py) to a saturated THF solution of (μ-Cl)$_2$[Cu(THF)(CNAr^{Mes2})]$_2$, followed by storage at −35 °C for 3 d, afforded diffraction quality crystals of (μ-Cl)$_2$[Cu(py)(CNAr^{Mes2})]$_2$. Prolonged drying of (μ-Cl)$_2$[Cu(py)(CNAr^{Mes2})]$_2$ in vacuo resulted in the removal of coordinated pyridine.

Synthesis of (μ-Br)$_2$[Cu(THF)(CNAr^{Mes2})]$_2$. To a THF slurry of cuprous bromide (0.085 g, 0.59 mmol, 3 mL) was added a THF solution of CNAr^{Mes2} (0.200 g, 0.59 mmol, 1 equiv, 5 mL). The reaction mixture was allowed to stir for 1 h, after which all volatile materials were removed under reduced pressure. Dissolution of the resulting colorless residue in THF (3−4 mL) followed by filtration and storage at −35 °C for 48 h resulted in colorless crystals, which were collected and dried in vacuo. Yield: 0.133 g, 0.28 mmol, 46.8%. The coordinated THF ligands are observed to dissociate in C_6D_6 solution. ^{1}H NMR (500.3 MHz, C_6D_6, 20 °C): δ = 6.91 (t, 1H, J = 7 Hz, *p*-Ph), 6.85 (s, 4H, *m*-Mes), 6.78 (d, 2H, *m*-Ph), 2.20 (s, 6H, *p*-CH_3), 1.99 (s, 12H, *o*-CH_3) ppm. ^{13}C{^{1}H} NMR (100.6 MHz, $CDCl_3$, 20 °C): δ = 149.4 (*C*≡N), 140.3, 138.3, 135.3, 133.7, 129.7, 129.4, 129.3, 126.7, 21.5 (*p*-*C*H_3), 20.4 (*o*-*C*H_3) ppm. FTIR (KBr pellet) (ν_{CN}) 2139 cm^{-1} also 2946, 2917, 2856, 1613, 1457, 1414, 1377, 1032, 849, 805, 757 cm^{-1}. Prolonged drying in vacuo resulted in an analytically pure sample lacking coordinated THF. Anal. Calcd for $C_{25}H_{25}NCuBr$: C, 62.18; H, 5.22; N, 2.90. Found: C, 61.01; H, 5.26; N, 2.76.

Synthesis of (μ-I)$_2$[Cu(THF)(CNAr^{Mes2})]$_2$. To a THF slurry of cuprous iodide (0.112 g, 0.59 mmol, 5 mL) was added a THF solution of CNAr^{Mes2} (0.200 g, 0.59 mmol, 1 equiv, 5 mL). The reaction was stirred overnight before volatile materials were removed under reduced pressure. Dissolution of the resulting colorless residue in THF (5 mL) followed by filtration and storage at −35 °C for 60 h resulted in colorless crystals, which were collected and dried in vacuo. Yield: 0.178 g, 0.34 mmol, 57.0%. The coordinated THF ligands are observed to dissociate in C_6D_6 solution. ^{1}H NMR (500.3 MHz, C_6D_6, 20 °C): δ = 6.91 (t, 1H, J = 8 Hz, *p*-Ph), 6.88 (s, 4H, *m*-Mes), 6.80 (d, 2H, J = 8 Hz, m-Ph), 2.25 (s, 6H, *p*-CH_3), 2.02 (s, 12H, *o*-CH_3) ppm. ^{13}C{^{1}H} NMR (100.6 MHz, C_6D_6, 20 °C): δ = 148.7 (*C*≡N), 140.3, 138.1, 135.5, 133.7, 129.7, 129.4, 129.3, 126.5, 21.6 (*p*-*C*H_3), 20.5 (*o*-*C*H_3) ppm. FTIR (KBr pellets): (ν_{CN}) 2146 cm^{-1} also 2945, 2916, 2855, 1612, 1456, 1414, 1376, 1031, 848, 806, 757 cm^{-1}. Prolonged drying in vacuo resulted in an analytically pure sample lacking coordinated THF. Anal. Calcd for $C_{25}H_{25}NCuI$: C, 56.66; H, 4.76; N, 2.64. Found: C, 56.39; H, 4.79; N, 2.46.

Synthesis of ClCu(CNAr^{Mes2})$_2$. To a CH_2Cl_2 solution of cuprous chloride (0.073 g, 0.74 mmol, 2 mL) was added a CH_2Cl_2 solution of CNAr^{Mes2} (0.500 g, 1.47 mmol, 2 equiv, 10 mL). The reaction mixture was allowed to stir for 1 h, after which all volatile materials were removed under reduced pressure. Dissolution of the resulting colorless residue in CH_2Cl (5 mL) followed by filtration and storage at −35 °C for 36 h resulted in colorless crystals, which were collected and dried in vacuo. Yield: 0.377 g, 0.48 mmol, 65.8%. ^{1}H NMR (500.3 MHz, C_6D_6, 20 °C): δ = 6.92 (t, 2H, J = 8 Hz, *p*-PH), 6.82 (s, 8H, *m*-Mes), 6.80 (d, 4H, J = 8 Hz, *m*-Ph), 2.19 (s, 12H, *p*-CH_3), 2.01 (s, 24H, *o*-CH_3) ppm. ^{13}C{^{1}H} NMR (100.6 MHz, $CDCl_3$, 20 °C): δ = 147.9 (*C*≡N), 139.6, 138.2, 135.4, 133.2, 130.3, 129.8, 128.8, 125.2, 21.3 (*p*-*C*H_3), 20.2 (*o*-*C*H_3) ppm. FTIR (KBr pellets): (ν_{CN}) 2143 cm^{-1} also 2946, 2919, 2860, 1612, 1460, 1271, 1223, 1147, 1031, 852, 756, 637 cm^{-1}. FTIR (KBr windows, C_6D_6 solution): (ν_{CN}) 2138 cm^{-1}. Anal. Calcd for $C_{50}H_{50}N_2CuCl$: C, 77.20; H, 6.48; N, 3.60. Found: C, 76.90; H, 6.31; N, 3.42.

Synthesis of ICu(CNAr^{Mes2})$_3$. To a THF slurry of cuprous iodide (0.037 g, 0.20 mmol, 2 mL) was added a THF solution of CNAr^{Mes2} (0.200 g, 0.59 mmol, 3.0 equiv, 5 mL). The reaction was stirred for about 2 h before volatile materials were removed under reduced pressure. Dissolution of the resulting colorless residue in THF (5 mL) followed by filtration and storage at −35 °C for 48 h resulted in colorless crystals, which were collected and dried in vacuo. Yield: 0.170 g, 0.14 mmol, 70.3%. ^{1}H NMR (500.3 MHz, C_6D_6, 20 °C): δ = 6.92 (t, 3H, J = 8 Hz, *p*-Ph), 6.85 (s, 12H, *m*-Mes), 6.80 (d, 6H, J = 8 Hz, m-Ph), 2.20 (s, 18H, *p*-CH_3), 2.03 (s, 36H, *o*-CH_3) ppm. ^{13}C{^{1}H} NMR (100.6 MHz, C_6D_6, 20 °C): δ = 139.8, 137.7, 135.8, 134.1, 129.7, 129.4, 129.2, 126.8, 21.4 (*p*-*C*H_3), 20.6 (*o*-*C*H_3) ppm. FTIR (KBr pellets) (ν_{CN}) 2119 cm^{-1} also 2946, 2918, 2858, 1613, 1457, 1415, 1378, 1060, 1032, 850, 805, 756 cm^{-1}. Anal. Calcd for $C_{75}H_{75}N_3CuI$: C, 74.52; H, 6.25; N, 3.48. Found: C, 73.48; H, 6.31; N, 3.42.

Synthesis of [(THF)Cu(CNAr^{Mes2})$_3$]OTf. To a THF solution of (C_6H_6)[CuOTf]$_2$ (0.200 g, 0.40 mmol, 3 mL) was added a THF solution of CNAr^{Mes2} (0.820 g, 2.42 mmol, 6 equiv, 10 mL). The reaction mixture was allowed to stir for 1 h, after which all volatile materials were removed under reduced pressure. Dissolution of the resulting colorless residue in THF (5 mL) followed by filtration and storage at −35 °C for 12 h resulted in colorless crystals, which were collected and dried in vacuo. Yield: 0.749 g, 0.61 mmol, 76.4% in 4 crops. ^{1}H NMR (400.1 MHz, $CDCl_3$, 20 °C): δ = 7.66 (t, 3H, J = 8 Hz, *p*-Ph), 7.25 (d, 6H, J = 8 Hz, *m*-Ph), 6.83 (s, 12H, *m*-Mes), 2.23 (s, 18H, *p*-CH_3), 1.89 (s, 36H, *o*-CH_3) ppm. ^{13}C{^{1}H} NMR (100.6 MHz, $CDCl_3$, 20 °C): δ = 146.0 (*C*≡N), 139.7, 138.3, 135.5, 133.1, 131.8, 130.3, 128.7, 124.0, 21.2 (*p*-*C*H_3), 20.1 (*o*-*C*H_3) ppm. ^{19}F{^{1}H} NMR (282.3 MHz, $CDCl_3$, 20 °C): δ = −78.9 ppm. FTIR (KBr pellets) (ν_{CN}) 2160 cm^{-1} also 2946, 2919, 2860, 1612, 1460, 1271, 1223, 1147, 1031, 852, 756, 637 cm^{-1}. Prolonged drying in vacuo did not remove the coordinated molecule of THF. Anal. Calcd for $C_{80}H_{83}F_3N_3O_4SCu$: C, 73.73; H, 6.42; N, 3.22. Found: C, 73.46; H, 6.60; N, 3.00. Crystals of [(η^1-*C*-C_6H_6)Cu(CNAr^{Mes2})$_3$]OTf were obtained by slurrying [(THF)Cu(CNAr^{Mes2})$_3$]OTf in C_6H_6, removing all volatile materials in vacuo and then allowing a dilute C_6H_6 solution of the resulting colorless residue to stand at room temperature for several days.

Synthesis of CuCl(CNAr^{Mes2})$_2$ from [(THF)Cu(CNAr^{Mes2})$_3$]OTf and External Chloride Sources. (A) From LiCl: A THF solution of [(THF)Cu(CNAr^{Mes2})$_3$]OTf (0.028 g, 0.022 mmol, 2 mL) was added to a THF slurry of LiCl (0.005 g, 0.11 mmol, 5.0 equiv). The reaction mixture was stirred overnight and then all volatile materials were removed under reduced pressure. The resulting residue was subjected to two cycles of slurrying in Et_2O (2 mL) followed by evaporation. The mixture was then stirred for 2 h in C_6D_6 and filtered. Analysis by ^{1}H NMR spectroscopy (300.1 MHz) resulted in a spectrum identical to that obtained by addition of 1.0 equiv of CNAr^{Mes2} to pure CuCl(CNAr^{Mes2})$_2$.[61] Analysis of the

(61) See Supporting Information.

mixture by $^{19}F\{^1H\}$ NMR spectroscopy did not give rise to any signal. A solution FTIR spectrum acquired on the sample exclusively revealed resolved stretches attributable to both $CNAr^{Mes2}$ (2118 cm^{-1}) and $CuCl(CNAr^{Mes2})_2$ (2138 cm^{-1}). **(B)** From $[NBu_4]Cl$: A THF solution of $[(THF)Cu(CNAr^{Mes2})_3]OTf$ (0.020 g, 0.016 mmol) was added to a THF solution of $[NBu_4]Cl$ (0.004 g, 0.015 mmol. 1.0 equiv). The reaction mixture was stirred overnight and then all volatile materials were removed under reduced pressure. The resulting residue was subjected to two cycles of slurrying in *n*-pentane (2 mL) followed by evaporation. The mixture was then stirred for 2 h in C_6D_6 and filtered. Spectroscopic analysis was identical to that described for treatment of $[(THF)Cu(CNAr^{Mes2})_3]OTf$ with LiCl.[61]

Crystallographic Structure Determinations. Single-crystal X-ray structure determinations were carried out at 100(2) K on either a Bruker P4 or Platform Diffractometer equipped with a Bruker APEX detector. Mo Kα radiation ($\lambda = 0.71073$ Å) was used in all cases. All structures were solved by direct methods with SIR 2004[62] and refined by full-matrix least-squares procedures utilizing SHELXL-97.[63] The crystallographic routine SQUEEZE[64] was used to account for disordered THF molecules of cocrystallization in the structures of $(\mu\text{-}Cl)_2[Cu(THF)(CNAr^{Mes2})]_2$, $(\mu\text{-}Br)_2[Cu(THF)(CNAr^{Mes2})]_2$ and $ICu(CNAr^{Mes2})_3$. Crystallographic data collection and refinement information are listed in Table 2.

Computational Details. DFT calculations were performed with the Amsterdam Density Functional (ADF) program suite,[65,66] version 2007.01.[67] For all atoms, the triple-ζ Slater-type orbital TZ2P ADF basis set was utilized without frozen cores. Relativistic effects were included by use of the zero-order regular approximation (ZORA).[68,69] The local density approximation of Vosko et al.[70] (VWN) was coupled with the generalized gradient approximation corrections described by Becke[71] and Perdew[72,73] for electron exchange and correlation, respectively. Crystallographic atomic coordinates were used as input where appropriate. Optimized geometries and molecular orbitals were visualized with the ADF-View graphical routine of the ADF-GUI.[74]

Acknowledgment. We gratefully acknowledge the UCSD Department of Chemistry and Biochemistry and the Camille and Henry Dreyfus New Faculty Awards Program for generous financial support. Professors Clifford P. Kubiak and Christopher C. Cummins are thanked for invaluable discussions.

Supporting Information Available: Representative ^1H NMR and FTIR spectra for exchange reactions, results of computational studies and crystallographic information files (CIF). This material is available free of charge via the Internet at http://pubs.acs.org.

IC8010986

(62) Burla, M. C.; Caliandro, R.; Camalli, M.; Carrozzini, B.; Cascarano, G. L.; De Caro, L.; Gaicovazzo, C.; Polidori, G.; Spagna, R. *J. Appl. Crystallogr.* **2005**, *38*, 381–388.
(63) Sheldrick, G. M. *Acta Crystallogr.* **2008**, *A64*, 112–122.
(64) van der Sluis, P.; Spek, A. L. *Acta Crystallogr.* **1990**, *A46*, 194–201.
(65) te Velde, G.; Bickelhaupt, F. M.; Baerends, E. J.; Fonseca Guerra, C.; van Gisbergen, S. J. A.; Snijders, J. G.; Ziegler, T. *J. Comput. Chem.* **2001**, *22*, 931–967.
(66) Fonseca Guerra, C.; Snijders, J. G.; te Velde, G.; Baerends, E. J. *Theor. Chem. Acc.* **1998**, *99*, 391–403.
(67) *ADF 2007.01*; SCM, Theoretical Chemistry, Vrije Universiteit: Amsterdam, The Netherlands; www.scm.com. Access date, October, 2007.
(68) van Lenthe, E.; Baerends, E. J.; Snijders, J. G. *J. Chem. Phys.* **1993**, *99*, 4597–4610.
(69) van Lenthe, E.; Snijders, J. G.; Baerends, E. J. *J. Chem. Phys.* **1996**, *105*, 6505–6516.
(70) Vosko, S. H.; Wilk, L.; Nusair, M. *Can. J. Phys* **1980**, *58*, 1200–1211.
(71) Becke, A. D. *Phys. Rev. A* **1988**, *38*, 3098–3100.
(72) Perdew, J. P. *Phys. Rev. B* **1986**, *33*, 8822–8824.
(73) Perdew, J. P. *Phys. Rev. B* **1986**, *34*, 7406–7406; Erratum.
(74) *ADF-GUI 2007.01*; SCM: Amsterdam, The Netherlands; www.scm.com. Access date, February, 2008.